Machine Learning Model For Predicting Anti-Dengue Drugs: A Three-Dimensional Quantitative Structure–Activity Relationship (3D QSAR) Study

Ali Qusay Khalid, Vasudeva Rao Avupati, Husniza Hussain

Abstract: Over the last five decades, dengue virus (DENV) emerged epidemically in many countries of the world which particularly located in tropical and sub-tropical areas. The elevation of its incidence up to 30-fold causing 50-100 million of dengue fever (DF) cases across the global in more than 100 countries. Due to this vast prevalence almost half of the population in the tropical and sub-tropical regions in the world are at risk of causing infection. There exist very few studies reported in developing machine learning three-dimensional quantitative structure-activity relationship (3D QSAR) modelling on anti-dengue compounds. Hence, in this study, a series of substituted 1,3,4-oxadiazole derivatives with corresponding anti-dengue activities were considered as ligand data set to develop and validate Schrodinger Phase™ 3D QSAR model based on the atoms present in the molecules forming the dataset. Further, this model was exposed to elucidate the relationship between structural features and anti-dengue activities. The established 3D QSAR model is statistically significant ($R^2_{\text{Training Set}}$ = 0.73 Q^2 ($R^2_{\text{Test Set}}$) = 0.78) with good predictive power. In addition, combined effects contour maps (blue: positive potential & red: negative potential) of this model were critically analyzed and elucidated the pharmacophore features responsible for the observed anti-dengue activities. The pharmacophore model mapped in this study is used as a directive tool for virtual screening and to identify new in silico hits in anti-dengue drug discovery and development pipeline.

Index Terms: Drug Discovery, Machine Learning, Atom-Based 3D QSAR, Anti-Dengue Drugs, Combined Effects Contour Maps.

1 INTRODUCTION

Dengue is the widespread viral infection transmitted between humans and primates by female Aedes vectors, it is a mosquito-borne disease principally through Aedes aegypti mosquito, which finds the tropical and sub-tropical areas suitable habitats for its development [1]. Dengue infection commences as an acute febrile disease-causing Dengue Fever (DF) that can be developed, with some patients, into a life-threatening illness called Dengue Shock Syndrome (DSS) as a consequence to Dengue Hemorrhagic Fever (DHF) [2]. DF is classified at the top of the seventeen “Neglected Tropical Diseases” (NTDs) by the World Health Organization (WHO) [3]. Epidemiologically, it is estimated that 390 million cases of dengue infection occurring annually, and nearly 2.4 billion people (about 40% of the world's population) are at the risk line [4]. The infection caused by a Flaviviridae virus family known to be termed as Dengue Virus (DENV) consisted of at least four serotypes (DENV-1, DENV-2, DENV-3 and DENV-4) [5]. The dengue virus has been established by both endemic and epidemic transmission cycles maintaining its existence.

- *Corresponding author: Dr. Vasudeva Rao Avupati, Senior Lecturer, Principal Investigator & Research Supervisor, Department of Pharmaceutical Chemistry, School of Pharmacy, International Medical University, Malaysia. PH-60167567763. E-mail: vasudevaraoavupati@gmail.com*
- *First author: Mr. Ali Qusay Khalid, Postgraduate Student, MSc in Molecular Medicine, School of Postgraduate Studies, International Medical University, Malaysia. PH-+601127089558.E-mail: ali.gk89@gmail.com*
- *Co-author: Dr. Husniza Hussain, Research Officer, Co-Supervisor, Nutrition Unit, Nutrition, Metabolism & Cardiovascular Research Centre, Institute for Medical Research, National Institutes of Health, Malaysia. E-mail: husnizah9thesis@gmail.com*

The structure of DENV consists of two components, the “structural” proteins (envelope protein, M protein and capsid) which order the overall confirmation of the virus and “non-structural” proteins (NS1, NS2A, NS2B, NS3, NS4A, NS4B and NS5) that plays a critical enzyme activity as a key role [6,7]. As a result, several protein targets of DENV have been identified [8], such as dengue virus protease (NS2B-NS3pro), RNA-dependent RNA polymerase (RdRp), methyltransferase (MTase), envelope protein (Ep), and helicase (NS3 helicase). These targets of high-resolution crystal structures enable researchers using virtual simulation to identify anti-dengue compounds throughout several machine learning techniques like 3D-QSAR and 3D pharmacophore modelling [9].

In the recent decade, diverse range of synthetic ligands have reported as potential anti-dengue compounds such as 2-phenyl-5[(E)-2-(thiophen-2-yl)ethenyl]-1,3,4-oxadiazoles [10], 3-acyl-indole [11]; 7-azaindole [12]; (4-amidino)-L-phenylalanine-containing inhibitors [13]; 3-aryl-2-cyanoacrylamide [14]; diamide containing heterocycles [15]; imidazole 4,5-dicarboxamide [16]; N-alkyl-deoxynojirimycins [17]; 2-aroyl-3-arylquinoline derivatives [18]; 2,1-benzothiazine 2,2-dioxides [19]; phthalazinones [20]; β-carbolines [21]; 7-deazapurine nucleosides [22]; 1,2-benzisothiazol-3(2H)-one [23]; hybrid 1,3,4-oxadiazole [24]; curcuminoids [25]; azoles (posaconazole and itraconazole) [26]. As of today, there is no FDA approved drug to radically cure dengue infection. The main challenge upon developing safe and effective vaccination or antiviral agents against DENV is the different serotypes manifestation, making the preventive and supportive care measurements are the only current defending tools. However, since the research field began witnessing a tremendous advancement in Computer-Aided Drug Discovery (CADD), proteomics scientists started to explore the structure of DENV thoroughly until being well-characterized nowadays. Primarily, machine learning is being a significant approach to develop and validate the inhibitory properties of some potential lead

models and to explain their mode of action in order to improve ligands' potency. Three-dimensional Quantitative structure–activity relationships (3D QSAR) is a machine learning approach of computer-aided drug design (CADD) that creates virtual predictive models to determine quantities includes biological or the toxicological profile of experimental or virtual compound libraries. This allows the medicinal chemists to establish a correlation between structure of the molecules and their biological activity. The potential of 3D QSAR has been significantly enhanced in recent years by the development and application of atom-based 3D QSAR modelling strategy. The primary aim of this study was to develop and validate robust atom-based 3D QSAR models capable of predicting reliable biological activity for new molecules. This method integrates the pairing of atom to atom between the molecular conformations. This pairing between the molecules further allows the preselected atom positions considered for the best matching, this strategy may not be suitable for the molecules with different types of basic skeletons or dissimilar molecules, in which the atoms are different to select to pair with each other for similarity analysis. Hence, the development and validation of atom-based 3D QSAR models for the virtual screening of compound libraries for the identification of anti-dengue agents seem promising. In atom-based 3D QSAR modelling, ligands alignment and determination of their stable conformation are important steps to develop a model. The atom-based 3D QSAR models are comparatively more useful than the pharmacophore-based 3D QSAR models, since structural features other than the pharmacophores, such as atom-based steric features, are significant to the observed activity. The hypothesis of this study designed to develop an atom-based 3D QSAR model using reported anti-dengue ligands and validate the same model that possess power to predict novel ligands by in silico screening of virtual compound libraries as potential anti-dengue agents.

2 MATERIALS AND METHODS

2.1 Machine Learning Software Requirements

Schrödinger Drug Discovery Suite Phase™ (a machine learning software) along with Maestro a graphical user interface [28] was used for molecular modelling, three-dimensional structure drawing, ligand energy minimization [29] and atom-based 3D QSAR modelling steps [30].

2.2 Collection of Biological Activity Dataset for Schrödinger Phase™ Atom-based 3D QSAR Modelling Study

In the present study, the compound dataset from the reported literature as potential anti-dengue agents was collected and used for the development and validation of Phase™ atom-based 3D QSAR model. The dataset created based on homologous series of 21 novel 1,3,4-oxadiazole derivatives reported by Benmansour et al., 2016 as dengue virus inhibitors [10]. The chemical structures and anti-dengue activities of the selected dataset was showed in Tables 2-3.

2.3 Curation (Chemical/Biological) of Dataset for Schrödinger Phase™ Atom-based 3D QSAR Modelling Study

Curation is a major integral step in atom-based 3D QSAR modelling. Although, the carefully chosen dataset is a potential resource for development of an atom-based 3D QSAR model, normally this data set could not be used directly for modelling purposes due to the presence of data set sampling errors. In order to construct a reliable and standardized atom-based 3D QSAR model, the selected dataset has been subjected for chemical and biological data curation using various types of curation filters which includes removal of mixtures, removal of inorganics, removal of salts, structure conversion cleaning, normalization of specific chemotype of compounds, removal of duplicate chemical structures, detection and verification of biological activity cliffs, removal of chirality/stereogenic isomers, molecular isotopes and pseudo-atoms and finally manual inspection of the ligand dataset. All the chemical structures of the curated dataset were further subjected to ligand preparation.

2.4 Preparation of Dataset for Schrödinger Phase™ Atom-based 3D QSAR Modelling Study

Ligand modelling was performed by sketching the two-dimensional (2D) molecular structures in a Schrödinger Maestro graphics platform interface using an embedded 2D Sketcher application. To identify 3D lower energy conformations of the ligands, all the compounds in the dataset were optimized using Schrödinger Maestro built-in graphical tool Ligprep application integrated with Optimized Potential for Liquid Simulations (OPLS_2015) force field. LigPrep is a Maestro built-in graphical tool that produces a single 3D lower-energy structure with fixed chiralities for every single processed input structure. The chemical structures of the prepared dataset both experimental and predicted activity data of the prepared model was showed in Table 2-3.

2.5 Selection of Training Set and Test Set for Schrödinger Phase™ Atom-based 3D QSAR Study

The prepared dataset initially divided into training and test sets with relative percentages of 75% and 25% respectively. The random selection tool integrated in Schrödinger Phase™ software was used to identify both training and test sets for the dataset.

2.6 Building of Schrödinger Phase™ Atom-based 3D QSAR Model Using Training Dataset

A definite analysis of ligand structural features of the selected dataset has been performed using atom-based 3D QSAR modelling. The pre-defined biological activities for both training set and test set were selected in a proper way that the diverse range of biological activities covering from low to high potencies. The structural features of the dataset have also been incorporated with the diverse range of substituents on the selected basic nucleus. In a 3D workspace, the structural alignment of the lower energy ligand conformations for the dataset were used to develop an atom-based predictive 3D QSAR model. The model was created for the selected datasets using training sets containing 16 (model compounds with a grid spacing of 1.0 Å. As a first step, the reported anti-dengue activities of the selected dataset were converted into their corresponding negative logarithmic values (pIC_{50} / pEC_{50}) values using the formula pIC_{50} = -log10 [IC_{50}] (or) pEC_{50} = -log10 [EC_{50}]. These values were used as dependent variables in the atom-based 3D QSAR modelling using Phase™ module of Schrodinger Discovery Suite software. Atom-based 3D QSAR model was interpreted by combined effects of contour maps. Areas covered with red and blue cubes indicate unfavorable and favorable regions respectively, to point toward

the anti-dengue activity of the dataset. The combined effects contour maps expose important features contributing towards ligands biological activity profile. In these contour maps, the blue cube regions represent favorable zones while red cube regions represent unfavorable zones for the biological activity. Visualizing atom-based 3D QSAR model developed in the present study by using various ligands from the dataset to gain insight about the relative contribution of each feature (D: hydrogen-bond donors; H: hydrophobic or nonpolar; N: negative ionic; P: positive ionic; W: electron-withdrawing and X: miscellaneous other atom types) in analyzing the biological activity. A graphical representation of the contour maps (cubes) generated for the most active and least active ligands in the developed 3D QSAR model. We have also considered different statistical parameters reported by Phase™ to evaluate and validate the atom-based 3D QSAR model developed in this study. The partial least squares regression (PLS regression) statistical method was used to construct a predictive model with a maximum of N/5 PLS factors (N is the total number of molecules present in the training set). The predictive 3D QSAR model which was found to be significant with a valid range of statistical parameters (showed in separate Tables under Results and Discussion). The best atom-based 3D QSAR model was validated by predicting the biological activities of the test sets. The predictive power of different QSAR model was identified using various statistical parameters such as Coefficient of determination (R^2); Coefficient of determination (Q^2) of the test set; Standard deviation (SD) of the regression; Root-mean squatted error (RMSE); Variance ration (F); Statistical significance (P); and Pearson correlation coefficient (Pearson-R) in order to select the best-fit model from the dataset, the combined information has been shown in Table 1.

2.7 Validation of the Predictive Ability of Schrödinger Phase™ Atom-based 3D QSAR Model Using Test Dataset

The ligands which have not been used to construct the atom-based 3D QSAR model were included in the external test set to validate -the developed model. Thus, statistics derived from both training set and test set were analyzed. The developed atom-based 3D QSAR model was also validated in parallel by the Y-randomization test (Scrambled activities) to confirm the robustness of the model. In the test, the dependent variable (biological activity data) has shuffled randomly and the new 3D QSAR model has been developed by using an independent variable framework. After multiple repetitions of this Test, the model was examined for their statistical significance. The low value of R^2 scramble test indicates that the QSAR model cannot fit random data, higher the value indicates that the variable dataset is complete, further can be considered as best fit model. To end with, the resulting R^2 and Q^2 values were used to confirm the stability of the model (Table 1).

3 RESULTS AND DISCUSSION

3.1 Alignment of Molecular 3D Conformations

The alignment of molecular 3D conformations is very vital for the development of a Schrödinger Phase™ atom-based 3D QSAR model. Thus, we used a template-ligand based alignment method. The most potent compound 10 of dataset was identified and used as template ligand and aligned to their respective database of training/test set molecules. The result of the alignment of conformations in a 3D-workspace is shown in the following Figures 1.

3.2 Schrödinger Phase™ Atom-based 3D QSAR Model

The results obtained for observed and predictive activities were presented in Tables 2 & 3. The predictive power of this model was analysed based on the predictability of the biological activities of the test molecules. The Q^2 (R^2_{Test}) was 0.7882 considered acceptable. The correlation plots between the experimental and the predicted (pIC_{50}) values of compounds in training set and test set of the atom-based 3D QSAR model developed from the dataset were depicted in Figure 2a-b. These results demonstrated that the anti-dengue activity predicted by the atom-based 3D QSAR model is in a good agreement with the experimental values with R^2 = 0.7353. Thus, the developed atom-based 3D QSAR model is reliable and can be applied to predict the activities of new derivatives belongs to this congeneric series in the future. Therefore, it was established that the resulting QSAR model has significance to predict the anti-dengue property with respect to the domain applicable to the observed bioassay. The reported anti-dengue activity was determined by using Pico Green® fluorescent DENV RdRp assay. This activity data forming part of the development and validation of our Schrödinger Phase™ atom-based 3D QSAR model 1. The activity data was considered as a dependent variable in the present study. The observed anti-dengue activity data was

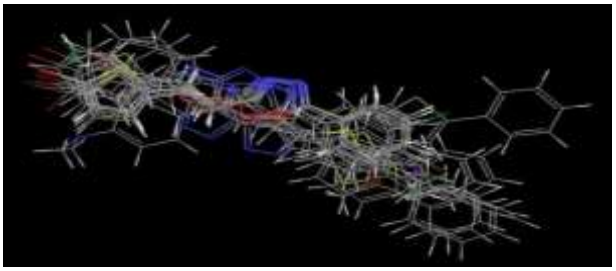

Fig. 1*. Structural alignment of the 3D ligand conformations for Schrödinger Phase™ atom-based 3D QSAR modelling: 3D alignment of the dataset (training/test).*

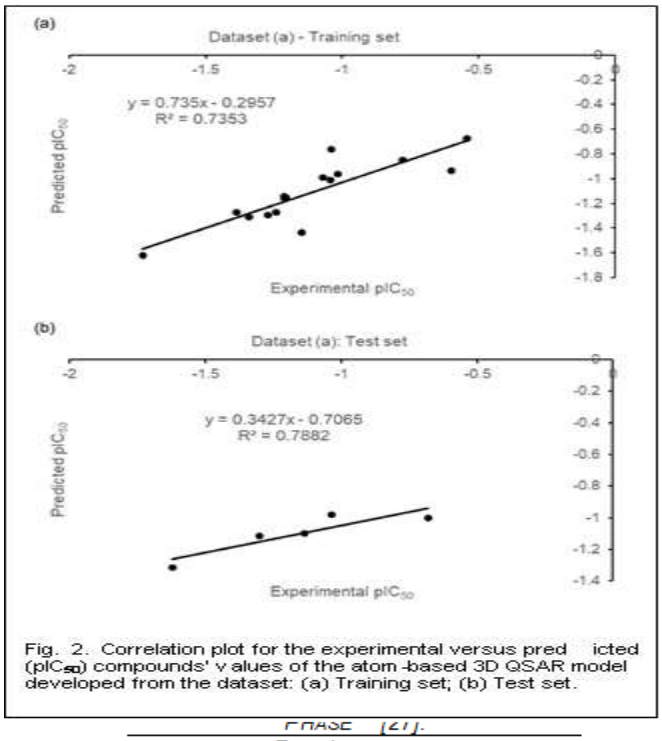

Fig. 2. Correlation plot for the experimental versus predicted (pIC_{50}) compounds' values of the atom-based 3D QSAR model developed from the dataset: (a) Training set; (b) Test set.

PHASE (27).

Statistical parameter	Results obtained Model Dataset	Analysis standards
m	3	n/5
n	16	n >15
R^2	0.7353	R^2>0.7
SD	0.1693	0.1-0.3
F	11.10	95%
P	0.000888	0.005 (5%)
R^2_{CV} ($R^2_{Scramble}$)	0.6556	>0.5
df_1	4	m+1
df_2	11	n-m-2
nT	5	nT = 25% of n
Q^2 (R^2_{Test})	0.7882	>0.5
$R^2_{Training}$ - Q^2	-0.0529	<0.3
RMSE	0.22	<0.5
Pearson-R	0.8877	>0.7

Number of PLS factors (m) included in the Schrödinger Phase™ atom-based 3D QSAR model; Number of molecules (n) included in the training set of Schrödinger Phase™ atom-based 3D QSAR model; Number of molecules (nT) included in the test set of Schrödinger Phase™ atom-based 3D QSAR model; Coefficient of determination (R^2); Coefficient of determination of the test set (Q^2); Standard deviation of the regression (SD); Root-mean squatted error (RMSE); Overall significance of the model (F) (variance ration); Statistical significance (P); Pearson correlation coefficient (Pearson-R); Degrees of freedom in model (df_1 (m +1)); Degrees of freedom in data (df_2 (n-m-2)).

used to carry out Schrödinger Phase™ atom-based 3D QSAR modelling study to develop a predictive model in order to identify the importance of different functional group present in the series of compounds tested. 1,3,4-oxadiazole scaffold substitution produced a series of molecules with potential anti-dengue properties. Analysis of the combined effects contour maps derived from the Schrödinger Phase™ atom-based 3D QSAR model is useful for understanding the direct correlation between the chemical structure and biological activity of active and inactive compounds among the series. Further, it is significant for identifying the areas where modifications will potentially affect the bioactivity. Excellent correlation in experimental and predicted activity was observed which indicates the correct selection of Schrödinger Phase™ atom-based 3D QSAR modelling as a computational approach in the present study. Compound 10 with 5-bromothiophe-2-ethenyl and 3,4-dichloro-phenyl substitutions at 2 and 5 positions of 1,3,4-oxadiazole ring is considered as a template compound with significant anti-dengue activity (IC_{50}: 3.5 ± 0.5 µM) as shown in Table 2. The compound 10 with relatively higher activity in the above series was further considered by the author for the synthesis of the next series of compounds to investigate the effect of substitutions on 1,3,4-oxadiazole ring system.As shown in Table 2, compounds 8,10, 12, 14, 16, 18, 20, 22, 24, and 25-28 were designed based on the general structure 1a of 1,3,4-oxadiazole using various substituent functional groups at positions 3, 4 and 5 of phenyl ring adjacent to it. Replacement of the bromo atom in compound 10 with phenyl group at 5 position of the thiophene exhibited a lower level of activity as seen in case of the compound 11. This observation has been supported by the contour maps generated from developed atom-based 3D QSAR model 1 Figure 3a-e.

As seen in case of compounds synthesized based on the general structure 2a, 17, 9, 13, 23, 15, 11, 21 and 19 with phenyl group at 5 position of the thiophene exhibited relatively lesser potencies than compound 10. This observation indicates that the presence of electron-releasing atom such as bromo substituent at 5 position of thiophene ring system enhances the bioactivity when compared to the electron-donating group such as phenyl ring system. From the data observed under each chemical scaffold modified with different R substituents showed a diverse range of activity profiles ranging from compounds with general structure 1a (IC_{50}: 3.5 to 20 µM) and general structure 2a (IC_{50}: 11.8 to 53.9 µM). However, it has been revealed that phenyl group attached to the position 2 of 1,3,4-oxadiazole basic nucleus is essential to maintain the activity. Correspondingly the contour maps of the Schrödinger Phase™ atom-based 3D QSAR model 1 also revealed the consistent information with respect to the areas covered with red and blue cubes in compound 10.

TABLE 2

ANTI-DENGUE ACTIVITY OF THE DATASET CONSISTING GENERAL STRUCTURE (1A), USED IN THE ATOM-BASED 3D QSAR MODELLING, COMPOUND CODES PRESENTED WERE SAME AS THE CODES REPORTED IN THE REFERENCE ARTICLE [10].

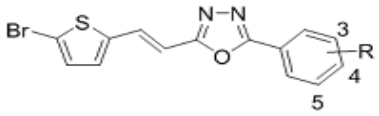

General structure (1a)

Code	R	Dataset	Exp. (μM)	Exp. pIC_{50}	Pred. pIC_{50}
8	3-Cl	Training	6.0	-0.778	-0.848725
10	3,4-Cl_2	Training	3.5	-0.544	-0.673031
12	4-F	Training	16.3	-1.212	-1.14169
14	4-OCH_3	Test	13.7	-1.137	-1.09689
16	4-CF_3	Test	4.8	-0.681	-1.00307
18	3-Br	Training	4.0	-0.602	-0.937868
20	4-$N(CH_3)_2$	Test	20.0	-1.301	-1.11721
22	H	Training	16.1	-1.207	-1.1542
24	4-Cl	Training	10.4	-1.017	-0.963222
25	4-Br	Test	10.9	-1.037	-0.978564
26	3-F	Training	16.3	-1.212	-1.15995
27	3,5-Cl_2	Training	11.0	-1.041	-0.764156
28	3-OCH_3	Training	11.1	-1.045	-1.01034

Thus, combined effects (hydrophobic/nonpolar, electron-withdrawing and others) contour maps around compound 10 that have reported the greater potency value are showed in Figures 3a. The blue colored contour maps observed in compound 10 has indicated the greater correlation with their experimental and predicted activities.

TABLE 3

ANTI-DENGUE ACTIVITY OF THE DATASET CONSISTING GENERAL STRUCTURE (2A), USED IN THE ATOM-BASED 3D QSAR MODELLING, COMPOUND CODES PRESENTED WERE SAME AS THE CODES REPORTED IN THE REFERENCE ARTICLE [10].

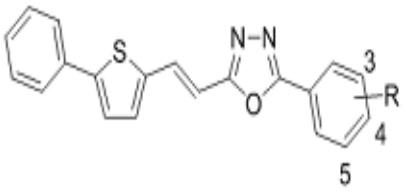

General structure (2a)

Code	R	Dataset	Exp. (μM)	Exp. pIC_{50}	Pred. pIC_{50}
9	3-Cl	Training	14.1	-1.149	-1.4386
11	3,4-Cl_2	Training	24.3	-1.386	-1.27152
13	4-F	Training	17.4	-1.241	-1.27307
15	4-OCH_3	Training	22.0	-1.342	-1.31352
17	4-CF_3	Training	11.8	-1.072	-0.990742
19	3-Br	Training	53.9	-1.732	-1.61995
21	4-$N(CH_3)_2$	Test	41.9	-1.622	-1.31642
23	H	Training	18.8	-1.27	-1.29407

The results obtained for observed and predictive activities were presented in Tables 2 & 3. The predictive power of this model was analysed based on the predictability of the biological activities of the test molecules. The Q^2 (R^2_{Test}) was 0.7882 considered acceptable. The correlation plots between the experimental and the predicted (pIC_{50}) values of compounds in training set and test set of the atom-based 3D

QSAR model developed from the dataset were depicted in Figure 2a-b. These results demonstrated that the anti-dengue activity predicted by the atom-based 3D QSAR model is in a good agreement with the experimental values with R^2 = 0.7353. Thus, the developed atom-based 3D QSAR model is reliable and can be applied to predict the activities of new derivatives belongs to this congeneric series in the future. Therefore, it was established that the resulting QSAR model has significance to predict the anti-dengue property with respect to the domain applicable to the observed bioassay. The reported anti-dengue activity was determined by using Pico Green® fluorescent DENV RdRp assay. This activity data forming part of the development and validation of our Schrödinger Phase™ atom-based 3D QSAR model 1. The activity data was considered as a dependent variable in the present study. The observed anti-dengue activity data was used to carry out Schrödinger Phase™ atom-based 3D QSAR modelling study to develop a predictive model in order to identify the importance of different functional group present in the series of compounds tested. 1,3,4-oxadiazole scaffold substitution produced a series of molecules with potential anti-dengue properties. Analysis of the combined effects contour maps derived from the Schrödinger Phase™ atom-based 3D QSAR model is useful for understanding the direct correlation between the chemical structure and biological activity of active and inactive compounds among the series. Further, it is significant for identifying the areas where modifications will potentially affect the bioactivity. Excellent correlation in experimental and predicted activity was observed which indicates the correct selection of Schrödinger Phase™ atom-based 3D QSAR modelling as a computational approach in the present study. Compound 10 with 5-bromothiophe-2-ethenyl and 3,4-dichloro-phenyl substitutions at 2 and 5 positions of 1,3,4-oxadiazole ring is considered as a template compound with significant anti-dengue activity (IC_{50}: 3.5 ± 0.5 µM) as shown in Table 2. The compound 10 with relatively higher activity in the above series was further considered by the author for the synthesis of the next series of compounds to investigate the effect of substitutions on 1,3,4-oxadiazole ring system. As shown in Table 2, compounds 8,10, 12, 14, 16, 18, 20, 22, 24, and 25-28 were designed based on the general structure 1a of 1,3,4-oxadiazole using various substituent functional groups at positions 3, 4 and 5 of phenyl ring adjacent to it. Replacement of the bromo atom in compound 10 with phenyl group at 5 position of the thiophene exhibited a lower level of activity as seen in case of the compound 11. This observation has been supported by the contour maps generated from developed atom-based 3D QSAR model 1 Figure 3a-e. As seen in case of compounds synthesized based on the general structure 2a, 17, 9, 13, 23, 15, 11, 21 and 19 with phenyl group at 5 position of the thiophene exhibited relatively lesser potencies than compound 10. This observation indicates that the presence of electron-releasing atom such as bromo substituent at 5 position of thiophene ring system enhances the bioactivity when compared to the electron-donating group such as phenyl ring system. From the data observed under each chemical scaffold modified with different R substituents showed a diverse range of activity profiles ranging from compounds with general structure 1a (IC_{50}: 3.5 to 20 µM) and general structure 2a (IC_{50}: 11.8 to 53.9 µM). However, it has been revealed that phenyl group attached to the position 2 of 1,3,4-oxadiazole basic nucleus is essential to maintain the activity. Correspondingly the contour maps of the Schrödinger Phase™ atom-based 3D QSAR model 1 also revealed the consistent information with respect to the areas covered with red and blue cubes in compound 10. Thus, combined effects (hydrophobic/nonpolar, electron-withdrawing and others) contour maps around compound 10 that have reported the greater potency value are showed in Figures 3a. The blue colored contour maps observed in compound 10 has indicated the greater correlation with their experimental and predicted activities.

3.3 Effects of functional groups (EWG/ERG) substituent's on the General structure (1a)

The reported bioactivity revealed that the compounds synthesized based on the general structure 1a were relatively more potent than the compounds synthesized based on the general structure 2a. Among the compounds tested, compounds with electron-withdrawing substituents at various substitution positions on the phenyl ring system exhibited comparatively additional potency than the compounds structures with electron-releasing substituents. In addition, a close look into the relationship between the type and specific position of the substituent functional group(s) explained the importance of electro-withdrawing and electron-releasing substituents towards the observed bioactivity, the results stated that the mono-substitution of electron-withdrawing group (halogen atoms such as Cl, Br, F) either at position 3 or position 4 remained favorable for the activity as seen in case of compounds 8 (3-Cl), 18 (3-Br), 26 (3-F), 24 (4-Cl), 25 (4-Br), 12 (4-F) and also 16 (4-CF_3) respectively. The electron-withdrawing halogens are relatively more effective than the alkyl substitutions. Similarly, the compounds mono-substituted with electron-releasing groups such as 4-OCH_3 in compound 14, 4-$N(CH_3)_2$ in compound 20 and 3-OCH_3 in compound 28 respectively were showed less potency at greater than >10 µM concentration. In comparison the compound 22 with unsubstituted phenyl ring exhibited more potency than the compound 20 with strong electron-releasing group. Its noteworthy to mention that the compound having electron-withdrawing groups di-substituted at position 3 and 4 of phenyl ring reported to be the most potent among the series of compounds screened by the author. The above observations were also being consistent with the combined effects contour maps generated based on the Schrödinger Phase™ atom-based 3D QSAR model as discussed under contour maps analysis and displayed in the Figures 3a-e.

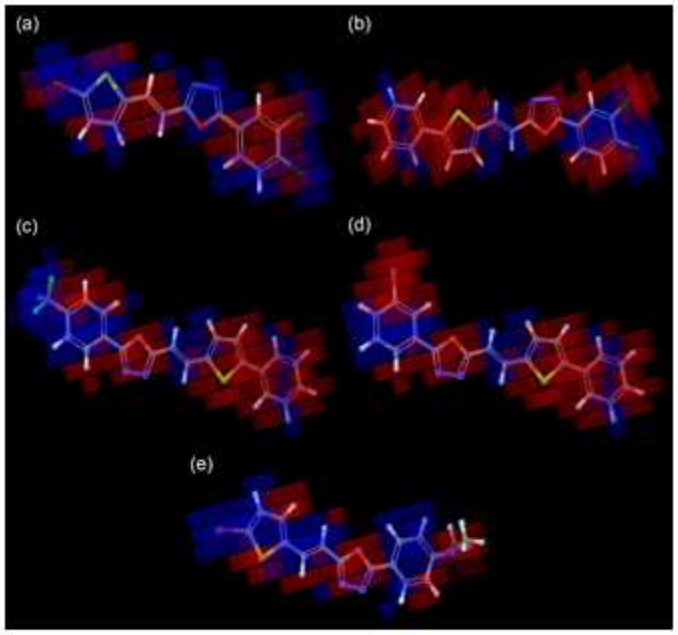

Fig. 3. Graphical representation of the combined effects (electron-withdrawing, hydrophobic/non-polar, and others) contour maps generated by Schrödinger Phase™ atom-based 3D QSAR model for the active and inactive compounds: (a) compound 10[1], (b) compound 11[1], (c) compound 17[1], (d) compound 19[1], (e) compound 20[1]. [1]Blue cubes indicate most favorable region for substitution, whereas Red cubes indicate unfavorable region for substitution with respect to the observed anti-dengue activity.

3.4 Effects of functional group (EWG/ERG) substituent's on the General structure (2a)

The most potent compound reported based on the general structure 2a was compound 17 consisting of electron-withdrawing group (CF_3) substituted at position 4 on the phenyl ring (> 10 µM). Pertaining to the potency of compounds, as seen in case of 23, an unsubstituted compound with no substitution either at position 3 or 4 on the phenyl ring exhibited better activity than the compound with 3,4-di-substituted with chlorine atom. In the similar manner, chlorine or fluorine atom substituted at positive 3 or 4 exhibited better activity than the bromo substitution on phenyl ring at position 3 has produced a compound with more negative potential. The two electron-donating groups 4-OCH_3 and 4-$N(CH_3)_2$ were exhibited least potency (> 20 µM) in comparison with the compound with no substitution either at position 3 or 4 on the phenyl ring. The above-mentioned correlation statements were also being predictive in the combined effects contour maps extracted based on the Schrödinger Phase™ atom-based 3D QSAR model as displayed in the Figure 3a-e.

3.5 Schrödinger Phase™ Atom-based 3D QSAR Model Combined Effects Contour Maps Analysis

The overall analysis of the combined effects contour maps generated based on the Schrödinger Phase™ atom-based 3D QSAR model comprising six different classes of atoms which includes D: hydrogen-bond donors; H: hydrophobic or nonpolar; N: negative ionic; P: positive ionic; W: electron-withdrawing and X: miscellaneous other atom types displayed in Figures 3a-e. The contour maps of these derivatives were carefully analyzed based on the red cubes and blue cubes which indicates positive and negative potentials of observed activities respectively. Through the interpretation of these contour maps. A blue contour map was seen around the phenyl ring at both 3 & 4 positions of the nucleus, indicating that phenyl group was well tolerable around this region. This was in good agreement with observed results, the observed results which also showed that dichloro substitution at 3 & 4 positions displayed potential effects against dengue virus as seen in case of compound 10. A blue colored contour map identified around the substituent at the 5 position of thiophene ring system indicated that the incorporation of functional group substituents at this position was more helpful to get good activity. This observation has also been in good agreement with the experimental. Likewise, a red colored contour map identified around the substituent at 5 position of thiophene ring system indicated that the presence of functional group substituents at this position was more useful to acquire negative contribution towards experimental anti-dengue activity as seen in case of compound 11 (Figure 3b).Sequentially, we have also examined the predictive ability of our model with respect to the estimation of the actual potency order of the compounds with experimental anti-dengue activities reported by the author. The order of predicted activities has also been in close agreement with the actual potency order of experimental activities. For example, the most active compound 10 related to the general structure 1a obtained in the experimental study has also been predicted as the most active compound by the atom-based 3D QSAR model 1 developed by us in this study, the combined effects contour map has depicted in Figure 3a. As shown in Figure 3a, a blue color contour was observed at the 5 position of thiophene ring in compound 10. Likewise, the most active compound 17 related to the general structure 2a obtained in the experimental study has also been predicted as the most active compound by our atom-based 3D QSAR model 1, the combined effects contour map has been showed in Figure 3c. As shown in Figure 3b, a red color contour was observed at the 5 position of thiophene ring, the presence of phenyl group at this position was not positively contributed towards anti-dengue activity. On the other hand, the least active compound among the series of compounds tested related to the general structure 1a and 2a was compound 19 obtained in the experimental study which was also been identified as the least active compound by our predictive atom-based 3D QSAR model, the combined effects contour map has been showed in Figure 3d. As shown in Figure 3e, a red color contour was observed at 5 position of thiophene ring, the presence of phenyl group at this position drastically reduced the anti-dengue activity. Additionally, the moderately active compound among the series of compounds tested related to the general structure 1a was compound 20 obtained in the experimental study which was maintained close order of potency as predicted by our atom-based 3D QSAR model, the combined effects contour map has been showed in Figure 3e. As shown in Figure 3a, a blue color contour was observed at 5 position of thiophene ring as in compound 10. In summary, based on the analysis of the combined effects (hydrophobic/non-polar, electron-withdrawing and others) contour maps of substituents at different positions of the general structure 1a & 2a developed using the datasets (training set and test set) of Schrödinger Phase™ atom-based 3D QSAR model, an optimized fingerprint pharmacophore was elucidated for identifying the 1,3,4-oxadiazole derivatives with anti-dengue properties is shown below in the Figure 4.

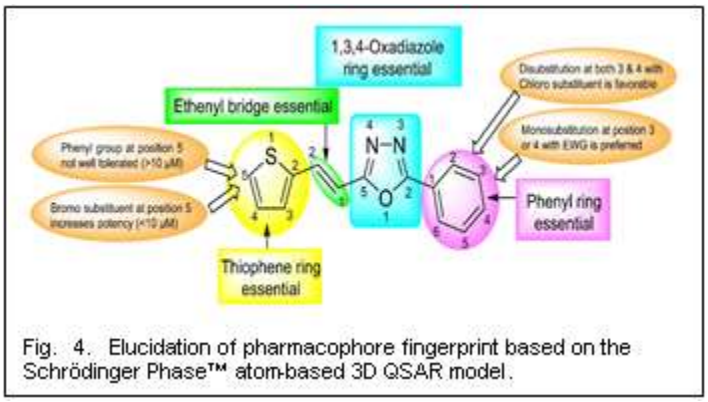

Fig. 4. Elucidation of pharmacophore fingerprint based on the Schrödinger Phase™ atom-based 3D QSAR model.

4 CONCLUSION

If In summary of the present study, we have successfully developed and validated Schrödinger atom-based 3D QSAR model using 1,3,4-oxadiazoles, derivatives as internal training and external test sets. This model has provided to be predictive with deeper insights into the chemical structural features responsible for their experimentally provided anti-dengue activities. Visualization of the combined effects contour maps of these atom-based 3D QSAR model with reference to the chemical structure of the molecules used in the study revealed the structural relationship with the bioactivity in all the cases. Based on these relationships we have carefully analyzed the structural features of the active compounds and inactive compounds among the series through an interpretation of combined effects contour maps with positive (blue contour) and negative (red contour) potentials and elucidated 2D pharmacophore model to design new ligands with anti-dengue properties. The 2D pharmacophore model derived from the above atom-based 3D QSAR model could be used as a general computational reference standard to develop a new virtual 1,3,4-oxadiazole containing ligands hypothesised to be as potential anti-dengue agents.

ACKNOWLEDGMENT

This research was funded by International Medical University (IMU) Joint-Committee on Research & Ethics, Project ID No: MMM I/2019(03)". One of the authors, Mr. Ali Qusay Khalid is thankful to the IMU Institute for Research Development & Innovation and Dean, IMU School of Pharmacy, & School of Post Graduate studies for providing software facilities to complete his final year research project for the fulfilment of the award of Master of Science in Molecular Medicine at IMU.

REFERENCES

[1] C. P. Simmons, J. J. Farrar, N. van Vinh Chau, and B. Wills, "Dengue," New England Journal of Medicine, vol. 366, no. 15, pp. 1423–1432, 2012.

[2] R. Edelman and J. Hombach, "'Guidelines for the clinical evaluation of dengue vaccines in endemic areas': Summary of a World Health Organization Technical Consultation," Vaccine, vol. 26, no. 33, pp. 4113–4119, 2008.

[3] P. J. Hotez et al., "Control of neglected tropical diseases," New England Journal of Medicine, vol. 357, no. 10, pp. 1018–1027, 2007.

[4] S. Bhatt et al., "The global distribution and burden of dengue," Nature, vol. 496, no. 7446, pp. 504–507, 2013.

[5] D. Normile, Surprising new dengue virus throws a spanner in disease control efforts. American Association for the Advancement of Science, 2013.

[6] N. Frimayanti, C. F. Chee, S. M. Zain, and N. A. Rahman, "Design of new competitive dengue Ns2b/Ns3 protease inhibitors—a computational approach," International journal of molecular sciences, vol. 12, no. 2, pp. 1089–1100, 2011.

[7] R. J. Kuhn et al., "Structure of dengue virus: implications for flavivirus organization, maturation, and fusion," Cell, vol. 108, no. 5, pp. 717–725, 2002.

[8] Behnam MAM, Nitsche C, Boldescu V, Klein CD. The Medicinal Chemistry of Dengue Virus. J Med Chem. 2016 Jun 23;59(12):5622–49.

[9] H. Berman, K. Henrick, and H. Nakamura, "Announcing the worldwide protein data bank," Nature Structural & Molecular Biology, vol. 10, no. 12, pp. 980–980, 2003.

[10] F. Benmansour et al., "Novel 2-phenyl-5-[(E)-2-(thiophen-2-yl) ethenyl]-1, 3, 4-oxadiazole and 3-phenyl-5-[(E)-2-(thiophen-2-yl) ethenyl]-1, 2, 4-oxadiazole derivatives as dengue virus inhibitors targeting NS5 polymerase," European journal of medicinal chemistry, vol. 109, pp. 146–156, 2016.

[11] D. Bardiot et al., "Discovery of indole derivatives as novel and potent dengue virus inhibitors," Journal of medicinal chemistry, vol. 61, no. 18, pp. 8390–8401, 2018.

[12] S. Verdonck et al., "Synthesis and Structure–Activity Relationships of 3, 5-Disubstituted-pyrrolo [2, 3-b] pyridines as Inhibitors of Adaptor-Associated Kinase 1 with Antiviral Activity," Journal of medicinal chemistry, vol. 62, no. 12, pp. 5810–5831, 2019.

[13] L. F. Weigel, C. Nitsche, D. Graf, R. Bartenschlager, and C. D. Klein, "Phenylalanine and phenylglycine analogues as arginine mimetics in dengue protease inhibitors," Journal of medicinal chemistry, vol. 58, no. 19, pp. 7719–7733, 2015.

[14] C. Nitsche, C. Steuer, and C. D. Klein, "Arylcyanoacrylamides as inhibitors of the Dengue and West Nile virus proteases," Bioorganic & medicinal chemistry, vol. 19, no. 24, pp. 7318–7337, 2011.

[15] M. Saudi et al., "Synthetic strategy and antiviral evaluation of diamide containing heterocycles targeting dengue and yellow fever virus," European journal of medicinal chemistry, vol. 121, pp. 158–168, 2016.

[16] M. Saudi et al., "Synthetic strategy and antiviral evaluation of diamide containing heterocycles targeting dengue and yellow fever virus," European journal of medicinal chemistry, vol. 121, pp. 158–168, 2016.

[17] Y. Du et al., "N-Alkyldeoxynojirimycin derivatives with novel terminal tertiary amide substitution for treatment of bovine viral diarrhea virus (BVDV), Dengue, and Tacaribe virus infections," Bioorganic & medicinal chemistry letters, vol. 23, no. 7, pp. 2172–2176, 2013.

[18] C.-H. Tseng et al., "Synthesis, antiproliferative and anti-dengue virus evaluations of 2-aroyl-3-arylquinoline derivatives," European journal of medicinal chemistry, vol. 79, pp. 66–76, 2014.

[19] R. Cannalire et al., "Functionalized 2, 1-benzothiazine 2, 2-dioxides as new inhibitors of Dengue NS5 RNA-dependent RNA polymerase," European journal of medicinal chemistry, vol. 143, pp. 1667–1676, 2018.

[20] D. Lu et al., "Discovery and optimization of phthalazinone derivatives as a new class of potent dengue virus inhibitors," European journal of medicinal chemistry, vol. 145, pp. 328–337, 2018.

[21] V. M. Quintana, L. E. Piccini, J. D. P. Zénere, E. B. Damonte, M. A. Ponce, and V. Castilla, “Antiviral activity of natural and synthetic β-carbolines against dengue virus,” Antiviral research, vol. 134, pp. 26–33, 2016.
[22] F. Yokokawa et al., “Discovery of potent non-nucleoside inhibitors of dengue viral RNA-dependent RNA polymerase from a fragment hit using structure-based drug design,” Journal of medicinal chemistry, vol. 59, no. 8, pp. 3935–3952, 2016.
[23] H. Lai et al., “Design, synthesis and characterization of novel 1, 2-benzisothiazol-3 (2H)-one and 1, 3, 4-oxadiazole hybrid derivatives: potent inhibitors of Dengue and West Nile virus NS2B/NS3 proteases,” Bioorganic & medicinal chemistry, vol. 21, no. 1, pp. 102–113, 2013.
[24] S. P. Lim et al., “Ten years of dengue drug discovery: progress and prospects,” Antiviral research, vol. 100, no. 2, pp. 500–519, 2013.
[25] Balasubramanian A, Pilankatta R, Teramoto T, Sajith AM, Nwulia E, Kulkarni A, et al. Inhibition of dengue virus by curcuminoids. Antiviral Research. 2019 Feb 1;162:71–8.
[26] F. Meutiawati et al., “Posaconazole inhibits dengue virus replication by targeting oxysterol-binding protein,” Antiviral research, vol. 157, pp. 68–79, 2018.
[27] R. Veerasamy, H. Rajak, A. Jain, S. Sivadasan, C. P. Varghese, and R. K. Agrawal, “Validation of QSAR models-strategies and importance,” Int. J. Drug Des. Discov, vol. 2, no. 3, pp. 511–519, 2011.
[28] S. Release, “1: Maestro,” Schrödinger, LLC, New York, NY, vol. 2017, 2017.
[29] S. Release, “2: LigPrep, Schrödinger, LLC, New York, NY, 2017,” New York, NY, 2017.
[30] S. L. Dixon, A. M. Smondyrev, and S. N. Rao, “PHASE: a novel approach to pharmacophore modeling and 3D database searching,” Chemical biology & drug design, vol. 67, no. 5, pp. 370–372, 2006.